Journal of Engineering Physics and Thermophysics, Vol. 80, No. 6, 2007

MATHEMATICAL MODEL OF HEAT TRANSFER IN THE U-SHAPED BLOCK OF THE UNPRESSURIZED DEVICE COMPARTMENT OF A GEOSTATIONARY SPACECRAFT

V. A. Burakov,[*] E. N. Korchagin,[a] V. P. Kozhukhov,[a] A. S. Tkachenko,[b] and I. V. Shcherbakova[c]

UDC 629.78.048.7.001.24

A new dynamic mathematical distributed-lumped parameter model of heat transfer in the U-shaped block of the service-system module of the unpressurized device compartment of a promising geostationary orbiting spacecraft having a long service life is proposed. A computational algorithm and software for calculating the multidimensional nonstationary temperature fields arising in the process of operation of the airborne-equipment devices and the system of nonregulated heat pipes in the indicated block have been developed. Results of calculation of these fields are presented.

Promising new-generation geostationary spacecraft having a long service life (not less than 12 years) include an unpressurized device compartment representing a block-module arrangement that simultaneously performs force and heat functions and protects the spacecraft from the action of outer-space factors. This compartment is shaped as a parallelepiped consisting of large-dimension, plane three-layer honeycomb panels and blocks of Π-, H-, and U-shaped configuration (respectively, for the payload, informative-logical, and power-engine modules) (Fig. 1) [1]. In the Π- and U-shaped blocks of the payload module and the service-system module, the heat-loaded airborne equipment (AE) is positioned on the panels-radiators oriented, in the orbiting regime, to the north and south. The use of an unusual H-shaped block in the service-system module makes it possible to partially or completely use all four faces of the unpressurized device compartment (instead of two — the north and south faces — as in all modern spacecraft). The temperature regime of the AE devices of the payload and service-system modules is provided by a passive thermal-regulation system including heat pipes, optical coatings, and electric heaters.

Because of the absence of sufficient experience in designing the apparatus being considered, the limited possibilities of their experimental study, and the necessity for a substantial decrease in the material costs, of importance is mathematical simulation of the thermophysical processes occurring in the blocks and modules of the unpressurized device compartment of a spacecraft in different regimes of its use, the contact heat exchange, the heat transfer in the AE devices, the conductive heat transfer in the three-layer honeycomb panels, and the heat and mass transfer in the heat pipes with account for the specificity of their laying and functioning in the panels of the payload and service-system modules.

The aim of the present work is to develop a new dynamic mathematical distributed-lumped parameter model of heat transfer in the U-shaped block of the service-system module, including a passive thermal-regulation system based on nonregulated low-temperature heat tubes, of the unpressurized device compartment of a geostationary spacecraft operating in the orbiting regime.

The device-radiator "north" and "south" panels are illuminated in the periodic six-month cycle by the Sun. At the winter-solstice point, the "north" panel is constantly shaded, while the "south" panel is constantly subjected to the action of direct solar radiation. After the six months, at the summer-solstice point, the panels change places in the sense of their illumination by the Sun. If the shades, reemissions, and rarefactions of the adjacent elements of the complex spacecraft arrangement, calling for a special comprehensive analysis, are not taken into account, the density of the solar-radiation flux $q_s(t)$ absorbed by the device-radiator "north" and "south" panels of the service-system mod-

[*] Deceased.

[a] Acad. M. F. Reshetnev Scientific-Production Company of Applied Mechanics, Zheleznogorsk, Russia; [b] Tomsk State Pedagogical University, Russia; [c] Scientific-Research Institute of Applied Mathematics and Mechanics, Tomsk University, 36 Lenin Ave., Tomsk, 634050, Russia; email: gla@niipmm.tsu.ru. Translated from Inzhenerno-Fizicheskii Zhurnal, Vol. 80, No. 6, pp. 9–17, November–December, 2007. Original article submitted June 7, 2006.

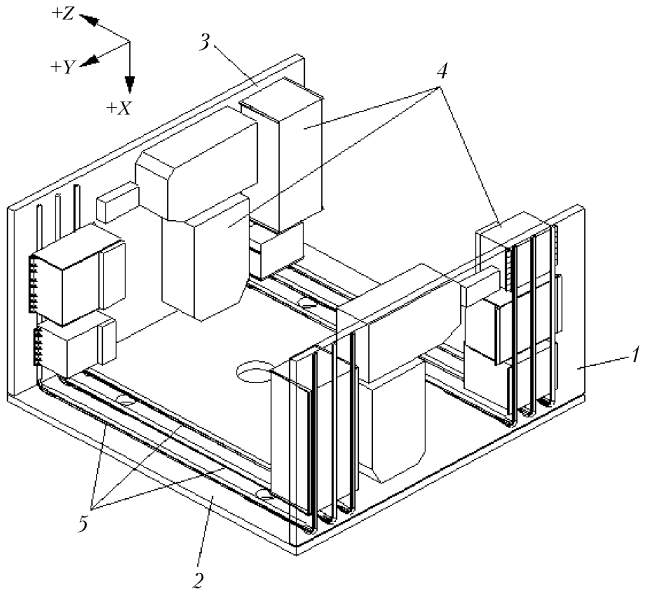

Fig. 1. Block-module arrangement of the unpressurized device compartment of a geostationary spacecraft and diagram of the typical laying of heat pipes in it: 1, 2, 3) honeycomb "south", "central", and "north" panels; 4) airborne equipment; 5) heat pipes. *XYZ*, global coordinate system.

ule in the six-month cycle is defined by a piecewise-continuous function accounting for the area of shade on the Earth at the vernal-equinox and autumnal-equinox points [2]:

$$q_{\mathrm{s}}(t) = \begin{cases} A_{\mathrm{s}} S_0 \cos\theta\,, & 0 < t \le t_{\mathrm{ES}}\,; \\ 0\,, & t_{\mathrm{ES}} < t \le 24\ \mathrm{h}\,. \end{cases} \tag{1}$$

The most important parameter in (1) is the ability of the special "optical solar reflector," representing a thermal-regulation coating applied on the surface of the device-radiator "north" and "south" panel, to absorb direct solar radiation. The dimension of this coating changes with time depending on the degree of its degradation under the action of outer-space factors; it becomes equal to $A_{\mathrm{s}} = 0.33$–0.4 at the end of the 12–15-year period of active existence of a promising geostationary spacecraft having a long service life. The density of radiation emitted by the radiative surfaces of the device-radiator "north" and "south" panels of the U-shaped block of the service-system module is determined by the Stefan–Boltzmann law.

Mathematical simulation of the conductive heat transfer in the three-layer ("north," "south," and "central") honeycomb panels of the U-shaped block of the service-system module is performed with the following assumptions:

1. The nonstationary temperature fields of the honeycomb panels of the blocks and modulus of the unpressurized device compartment are calculated separately in their own local Cartesian coordinate system, where the 0*Z* axis is always directed inside.

2. The temperature gradient in the thickness of the high-heat-conductivity metal casings of the honeycomb panels is disregarded (the approximation of a thermally thin wall).

3. The temperature gradients in the thickness and along the height of the carcass elements are disregarded.

4. The honeycomb filler is considered as a continuous anisotropic (orthotropic) porous medium with good thermophysical properties. The radiative heat exchange is disregarded.

5. The thermophysical characteristics of the materials from which the panels being considered are made are assumed to be constant.

6. The model of heat transfer from the heat-loaded airborne equipment to the inner surface of the metal casing of a honeycomb panel includes boundary conditions of the second kind set at the locations of the devices and heat-release cyclograms.

With the above assumptions, the dynamic mathematical distributed-parameter model of heat transfer in the three-layer honeycomb "north," "south," and simple "central" (with no AE devices) panels of the U-shaped block of the service-system module will have the following form in the Cartesian coordinate system:

$$\frac{\partial T_m}{\partial t} = a_{\rm f}\left(\frac{\partial^2 T_m}{\partial x^2} + \frac{\partial^2 T_m}{\partial y^2}\right) + Q_m\,, \qquad (2)$$

$$m = 1, 2\,,\quad 0 < x < L_x\,,\quad 0 < y < L_y\,,\quad 0 < t \le 24 \text{ h}\,,$$

$$\frac{\partial T_m}{\partial t} = a_{\rm st}\frac{\partial^2 T_m}{\partial \xi^2} + \Phi_m + \Phi_{m\rm cont}\,,\quad m = \overline{3, 6}\,,\quad 0 < \xi < 2\,(L_x + L_y)\,,\quad 0 < t \le 24 \text{ h}\,, \qquad (3)$$

$$\left.\frac{\partial T_m}{\partial n}\right|_{\Gamma_m} = 0\,,\quad m = 1, 2\,, \qquad (4)$$

$$\left.\frac{\partial T_3}{\partial \xi}\right|_{\xi=0} = \left.\frac{\partial T_6}{\partial \xi}\right|_{\xi=2(L_x+L_y)}\,,\quad T_3\,|\,\xi=0 = T_6\,|\,\xi=2(L_x+L_y)\,, \qquad (5)$$

$$T_m\,(x, y, 0) = T_{\rm int}\,,\quad m = 1, 2\,,\quad 0 \le x \le L_x\,,\quad 0 \le y \le L_y\,, \qquad (6)$$

$$T_m\,(\xi, 0) = T_{\rm int}\,,\quad m = \overline{3, 6}\,,\quad 0 \le \xi \le 2\,(L_x + L_y)\,. \qquad (7)$$

The dynamic mathematical distributed-parameter model (2)–(7) defines the conductive heat transfer in the six main elements of a three-layer honeycomb panel: (2) defines the heat transfer in the supporting metal casings and (3) in the carcass elements, and (4)–(7) are boundary and initial conditions. The origin of coordinates $\xi = 0$ coincides with the origin of the Cartesian coordinate system. The carcass elements are numbered in the direction of the $0Y$ axis. The boundary condition (5) corresponds to the periodic problems on nonstationary heat conduction.

The dynamic model (2)–(7) is closed by expressions defining the source terms Q_m, Φ_m, and $\Phi_{m\rm cont}$ in the quasi-one-dimensional and quasi-two-dimensional equations of nonstationary heat conduction (2) and (3), which determine the features of the heat transfer in each of the three honeycomb panels of the U-shaped block of the service-system module:

$$Q_1 = \frac{\sum\limits_n q_{\rm s.e1}n + E_{\rm r1} - q_{\rm cond1} - \sum\limits_k q_{\rm h.p1}k - q_{\rm f.st1}}{\delta_{\rm f1}\rho_{\rm f}c_{\rm f}}\,, \qquad (8)$$

$$q_{\rm s.e}n = \frac{P_{\rm s.e}n\,(t)}{F_{\rm s.e}}\,,\quad n = \overline{1, N_{\rm s.e1}}\,,\quad n = \overline{1, N_{\rm s.e3}}\,,$$

$$q_{\rm h.p1}k\,(x, y, t) = \alpha_{\rm f.p}k\,[T_1\,(x, y, t) - T_{\rm v}k\,(t)]\,,\quad k = \overline{1, N_{\rm h.p}}\,,$$

$$q_{\rm f.st1} = \alpha_{\rm f.st}\,[T_1\,(0, y, t) + T_1\,(x, L_y, t) + T_1\,(L_x, y, t) + T_1\,(x, 0, t) - (T_3 + T_4 + T_5 + T_6)]\,,$$

$$Q_2 = \frac{q_s(t) + q_{cond2} - \varepsilon_2 \sigma_0 T_2^4 - q_{f.st2}}{\delta_{f2} \rho_f c_f}, \tag{9}$$

$$q_{cond1} = q_{cond2} = \frac{\lambda_{eff}}{\delta_h} \left(\frac{Bi_{f.h}}{2 + Bi_{f.h}} \right) (T_1 - T_2),$$

$$q_{f.st2} = \alpha_{f.st} [T_2(0, y, t) + T_2(x, L_y, t) + T_2(L_x, y, t) + T_2(x, 0, t) - (T_3 + T_4 + T_5 + T_6)],$$

$$\Phi_3 = \frac{\alpha_{f.st} [T_1(0, y, t) + T_2(0, y, t) - 2T_3]}{h_{st} \rho_{st} c_{st}}, \tag{10}$$

$$\Phi_{3c} = -\frac{\alpha_c (\bar{T}_3 - \bar{T}_{3c})}{\delta_{st} \rho_{st} c_{st}}, \tag{11}$$

.....

$$\Phi_6 = \frac{\alpha_{f.st} [T_1(x, 0, t) + T_2(x, 0, t) - 2T_6]}{h_{st} \rho_{st} c_{st}}, \tag{12}$$

$$\Phi_{6c} = -\frac{\alpha_c (\bar{T}_6 - \bar{T}_{6c})}{\delta_{st} \rho_{st} c_{st}}, \tag{13}$$

where $\bar{T}_{mc}$ is the mean-integral temperature of the metal-casing zone that is opposite to the panel contacting with the mth element of the carcass.

Mathematical simulation of the heat transfer in the nonregulated single-leg heat pipes built into the anisotropic honeycomb filler found in the inner and outer casings of the U-shaped block of the service-system module of the unpressurized device compartment is performed, without considering the details of the hydrodynamics and the heat and mass transfer in the vapor channel, with the use of dynamic mathematical lumped-parameter models of conductive heat transfer of the type of the models described in [2] on the following assumptions:

(1) the three heat pipes thermally connecting the device-radiator "south" and "north" panels function in the prelimit regime with no hydrodynamic choking as well as ebullition and solidification of the heat-transfer agent;

(2) the heat transfer in the axial and peripheral directions of the heat-pipe elements is insignificant;

(3) the vapor is in the saturation state and its temperature distribution along the heat pipes remains unchanged;

(4) the dimensions of the evaporation and condensation zones of the heat pipes correspond to the longitudinal dimensions of the sites of location of the AE devices and the lengths of the zones of connection of two heat pipes in a bundle;

(5) the coefficients of heat transfer in the process of phase transformations of the heat-transfer agent in the evaporation and condensation zones of the heat pipes are constant.

The other assumptions being used are described in [2].

The dynamic lumped-parameter model of conductive heat transfer in a bundle of three heat pipes of the U-shaped block of the service-system module (see Fig. 1) represents the system of $4 + N_{s.e1} + N_{s.e3}$ ordinary differential equations of heat balance relative to the average temperatures in the characteristic zones of the heat pipes with corresponding initial conditions:

$$\sigma_{f.p1n} (T_{11n} - T_{e1n}) = C_{e1n} \frac{dT_{e1n}}{dt} + \sigma_{e11n} (T_{e1n} - T_{v1}), \tag{14}$$

$$\sigma_{c1}\,(T_{v1}-T_{c1})=C_{c1}\,\frac{dT_{c1}}{dt}+\sigma_{p.p12}\,(T_{c1}-T_{e2})\,,$$

$$T_{e1n}\,(0)=T_{c1}\,(0)=T_{int}\,,$$

$$\sigma_{p.p12}\,(T_{c1}-T_{e2})=C_{e2}\,\frac{dT_{e2}}{dt}+\sigma_{e2}\,(T_{e2}-T_{v2})\,, \tag{15}$$

$$\sigma_{f.p2n}\,(T_{12n}-T_{e2n})=C_{e2n}\,\frac{dT_{e2n}}{dt}+\sigma_{e22n}\,(T_{e2n}-T_{v2})\,,$$

$$\sigma_{c2}\,(T_{v2}-T_{c2})=C_{c2}\,\frac{dT_{c2}}{dt}+\sigma_{p.p23}\,(T_{c2}-T_{e3})\,,$$

$$T_{e2}\,(0)=T_{e2n}\,(0)=T_{c2}\,(0)=T_{int}\,,$$

$$\sigma_{p.p23}\,(T_{c2}-T_{e3})=C_{e3n}\,\frac{dT_{e3n}}{dt}+\sigma_{f.p3n}\,(T_{c3n}-T_{13n})\,, \tag{16}$$

$$\sigma_{c33n}\,(T_{v3}-T_{c3n})=C_{c3n}\,\frac{dT_{c3n}}{dt}+\sigma_{f.p3n}\,(T_{c3n}-T_{13n})\,,$$

$$T_{e3}\,(0)=T_{c3n}\,(0)=T_{int}\,.$$

The system of equations (14)–(16) is nonclosed because the temperature of the saturated vapor in the heat pipes is unknown. The closeness condition is formulated on the basis of the law of energy conservation in the vapor channel of a heat pipe in the known quasi-stationary form:

$$\sum_n \sigma_{e1}\,(T_{e1n}-T_{v1})+\sigma_{c1}\,(T_{c1}-T_{v1})=0\,, \tag{17}$$

$$\sigma_{e2}\,(T_{e2}-T_{v2})+\sum_n \sigma_{e22n}\,(T_{e2n}-T_{v2})+\sigma_{c2}\,(T_{c2}-T_{v2})=0\,, \tag{18}$$

$$\sigma_{e3}\,(T_{e3}-T_{v3})+\sum_n \sigma_{c33n}\,(T_{c33n}-T_{v3})=0\,. \tag{19}$$

The dynamic mathematical model (1)–(19) of heat transfer in the unusual U-shaped block (including heat-loaded airborne equipment) of the service-system module of the unpressurized device compartment of a geostationary spacecraft, developed in the real-physical-time scale for the conditions of orbiting operation, qualifies, according to the classification of [3], as a second-level model of heat transfer in which the heat state of the most important elements of the module and the passive thermal-regulation system is described with the use of distributed and lumped parameters. The mathematical model (1)–(9) allows one to determine the coordinate- and time-dependent multidimensional nonstationary temperature fields in the three-layer honeycomb ("south," "north," "central") panels of the U-shaped block of the service-system module and the temperature at the computational sites of the passive thermal-regulation system based on a net of nonregulated heat pipes in the case where the AE devices function in the 24-hour cycle of illumination by the Sun. The temperature fields determined are then used for estimation of extremum heat regimes of the airborne equipment by the maximum and minimum temperatures at the locations of the devices [2].

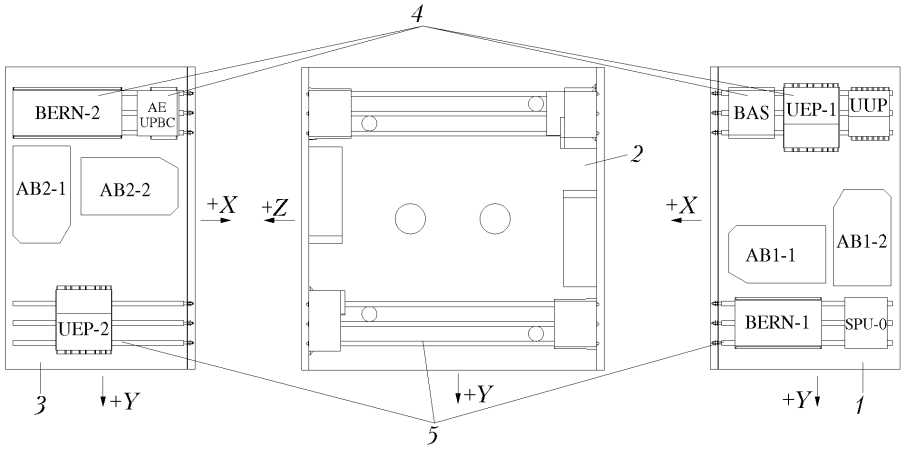

Fig. 2. Layout diagram of devices and laying of heat pipes on the panels of the power engine block. Designations 1–5 are identical to the designations in Fig. 1.

The quasi-two-dimensional nonstationary equations of heat conduction in the supporting casings (2) are realized numerically by the finite-difference method with the use of the iteration-free economical two-layer scheme of component-by-component splitting (fractional steps) with weights of N. N. Yanenko [4] and a fixed irregular grid. The quasi-one-dimensional nonstationary equations of heat conduction in the carcass elements (3), considered as a closed system, are numerically realized along the march coordinate with the use of the cyclic marching method [5]. The systems of the first-order ordinary differential equations (14)–(16) defining the current average temperatures in the evaporation, heat-transfer, and condensation zones of the heat pipes are numerically realized, after they are brought to the Cauchy problem, by implicit schemes of first or second order of accuracy. The calculations in each time layer are verified by control of the integral heat balance in the three-layer honeycomb panel, the local heat balances at the locations of the heat-realizing AE devices, and the integral heat balance in the bundles of heat pipes.

A version of the EDB1 computer program has been developed in the high-level Visual C++ (v.6.0) algorithmic language for IBM-compatible personal computers. In the 24-hour cycle, the typical time of computation of one variant by the EDB1 program with the use of finite-difference 31 × 57 ("south" panel), 39 × 44 ("north" panel), and 28 × 46 ("central" panel) grids with a time step τ = 20 sec (panels), τ = 0.1 (passive thermal-regulation system) on a Pentium-III personal computer comprises about 3 min, which is reasonably acceptable for the performance of multiparametric numerical calculations. In this case, the accuracy of estimation of the integral and local heat balances at the locations of the devices was not worse than 8.6%.

The results of numerical calculations of the nonstationary multidimensional temperature fields in the three-layer honeycomb panels and of the operating parameters of the heat pipes in the U-shaped block of the service-system module of the unpressurized device compartment were processed with the use of modern techniques of graphic and animated visualization and color computer animation. Numerical calculations of the nonstationary multidimensional temperature fields in the U-shaped block of the service-system module of a promising geostationary spacecraft of long service life with six bundles of three ammoniac heat tubes of one-leg profile with a cylindrical groove capillary structure, made from an AD-31-T5 aluminum alloy by State Standard 4784-74, were carried out by the EDB1 program, developed by us, on a Pentium-III personal computer for the case of functioning of the AE devices by the cyclograms. The conditions of orbiting of the spacecraft at the end of the 15-year period of its active existence (A_s = 0.4, θ = 66.5°) were determined at the vernal-equinox point (S_0 = 1400 W/m^2) in the case where the "south" panel was illuminated by the Sun for the period of time $0 < t \le 22.8$ h and the Earth was shaded for the period of time $22.8 < t \le 24$ h. The diagram of the airborne-equipment layout on the "south" and "north" device-radiator panels and the laying of heat pipes are shown in Fig. 2. The heat-release cyclograms of the AE devices in the U-like block of the service-system module are presented in Fig. 3. The following initial data were used:

linear dimensions of the "south" and "north" panel-radiators, 1.2 × 2.0 × 0.05 m;

thickness of the casings: $\delta_{f1} = \delta_{f2} = 10^{-3}$ m;

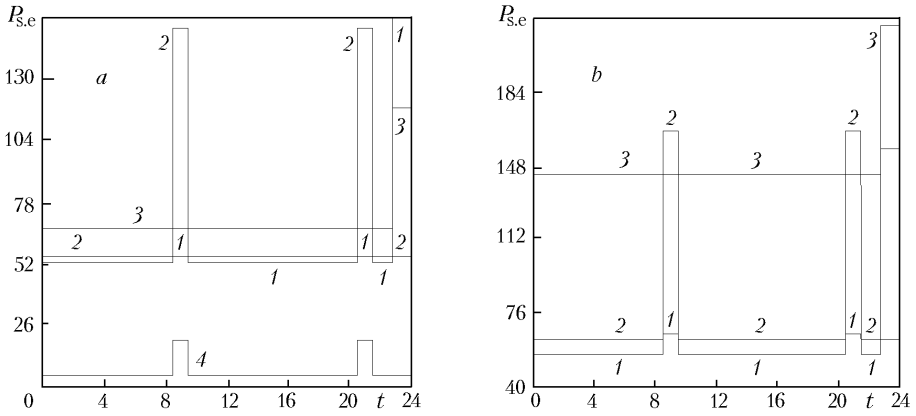

Fig. 3. Cyclograms of heat release by the devices of the "south" panel (a) [1) AB-1; 2) UEP-1; 3) BERN-1; 4) UUP] and the "north" panel (b) [1) AB-2; 2) UEP-2; 3) BERN-2]. $P_{s.e}$, W; t, h.

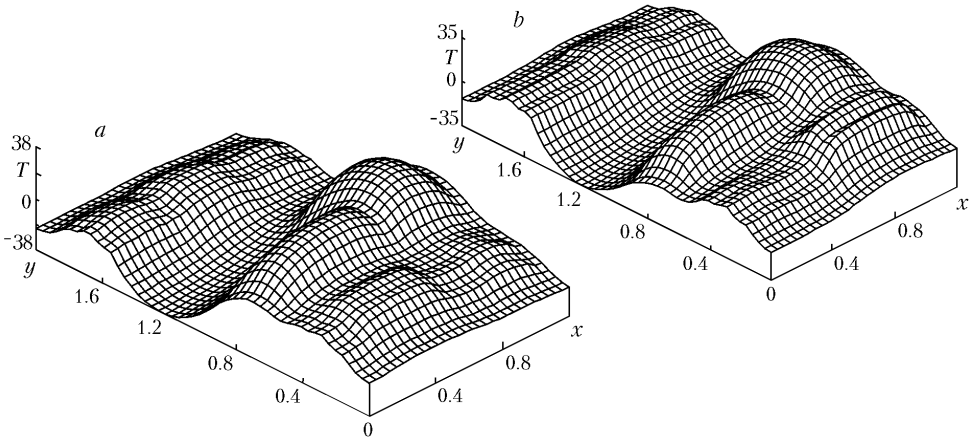

Fig. 4. Spatial distribution of the temperature fields of the metal casings of the "south" (a) and "north" (b) panels. T, °C; x, y, m.

thermophysical characteristics of the casing material: ρ_f = 2700 kg/m^3, λ_f = 130 W/(m·K), c_f = 880 J/(kg·K);

height of the honeycomb filler, $48\cdot10^{-3}$ m;

effective heat-conductivity coefficient of the honeycomb filler of all the panels, 1.48 W/(m·K) (thickness of the foil, $4\cdot10^{-5}$ m; size of the honeycomb cell, $5\cdot10^{-3}$ m; heat conductivity of the foil material, 130 W//(m·K));

parameters of the heat pipes: outer diameter, $14\cdot10^{-3}$ m; inner diameter, $12\cdot10^{-3}$ m; width of a leg, 0.03 m; mass, 0.31 kg/m; coefficient of heat transfer in the phase transformations in the evaporation and condensation zones, 7000 W/(m^2·K);

specific thermal resistance of the adhesive joint of the heat-pipe leg and the panel casing, $4\cdot10^{-3}$ m^2·K/W;

specific thermal resistance of the adhesive joint of the heat pipes through the legs, 10^{-3} m^2·K/W; length of the joint, 0.3 m;

specific thermal resistance of the adhesive joint between the casing and the honeycomb filler, 10^{-3} m^2·K/W;

specific thermal resistance of the adhesive joint of the casing and the carcass elements, 0.14 m^2·K/W;

specific thermal resistance of the contact between the two honeycomb panels, 0.02 m^2·K/W;

initial temperature, 273 K.

The results of numerical calculations of the nonstationary multidimensional temperature fields of the metal casing of the "south" and "north" device panels at the instant t = 24 h in the global coordinate system are shown in Fig. 4. As is seen, the isotherms are oriented along the heat pipes. On the "south" panel, the maximum temperature

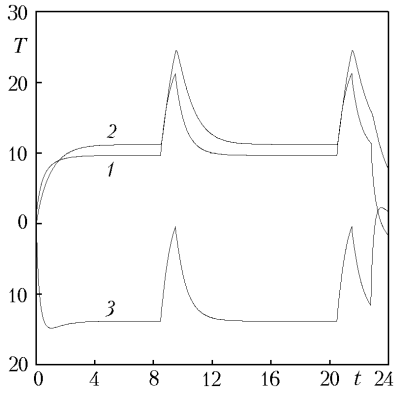

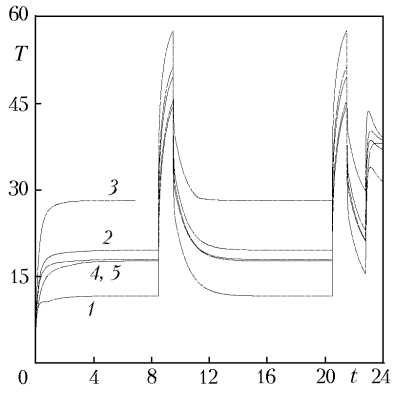

Fig. 5. Dynamics of the 24-hour change in the average temperatures of the metal casings of the honeycomb panels of the power engine block: 1) "south" panel; 2) simple "central" panel; 3) "north" panel. T, ^{o}C; t, h.

Fig. 6. Dependence of the dynamics of the 24-hour change in maximum temperatures at the locations of the AE devices on the "south" panel on different factors: A_s = 0.26 (1), 0.33 (2), and 0.4 (3); $\delta_f = 1.5 \cdot 10^{-3}$ m (4); ε_2 = 0.87 (5). T, ^{o}C; t, h.

(38.5^{o}C) is attained at the location of an AB1-2 device, the heat release of which, according to the cyclogram, is maximum at this instant of time. On the other hand, on the "south" panel, the largest amount of heat, according to the cyclogram, is released by the BERN-2 device, the temperature at the location of which is only 30.1^{o}C. The maximum temperature, equal to 40.9^{o}C, is attained at the location of an AB2-1 device, the heat release of which at this instant of time is somewhat smaller than that of the BERN-2 device, even though it is higher than the heat release of the other devices. This can be explained by the fact that heat pipes are absent under the AB2-1 device. In actuality, the maximum temperatures attained at these panels will be lower because of the internal radiative heat exchange arising in the process of operation of the U-like block of the service-system module. The largest isothermality of the temperature fields was attained at the locations of the devices the heat load of which was maximum at a given instant of time — 34.9^{o}C at the "north" panel and 37.8^{o}C at the "south" panel, under which there were no heat pipes. The temperature of the saturated vapor of the six links of a heat pipe ranged from –5.6 to +13^{o}C.

The dynamics of the 24-hour change in the average temperature of the metal casings of the honeycomb panels of the power engine block is shown in Fig. 5. According to the cyclograms, the highest temperatures are attained at the instants the total heat released by the devices is maximum, except for the "south" panel, where a peak at $t > 22$ h is absent. This is explained by the fact that, at this instant, the illuminated "south" panel becomes shaded and the total heat flux is decreased by the value of the direct solar-radiation flux. Due to the heat pipes, this effect is extended to the "central" panel. The dynamics shown in Fig. 5 completely corresponds to the processes occurring at the "north" panel because it is always shaded. The average temperature at the "central" panel is somewhat higher (of the order of 2^{o}) than that at the "south" panel because of the intensive removal of heat released by the devices of both the "south" and "north" panels through the heat pipes.

The dynamics of the 24-hour change in the maximum temperatures at the locations of the AE devices on the "south" panel, determined with account for the influence of different factors, is presented in Fig. 6. The maximum temperature is directly proportional to the coefficient of absorption of direct solar radiation. An increase in A_s from 0.26 to 0.4 causes an increase in the maximum temperature of the order of 15^{o}C. An increase in the thickness of the casings by a factor of one and a half causes a decrease in the maximum temperature by 1.5^{o}C in the periods of time corresponding to the smooth portions of the temperature dependence and more than 3^{o}C at its peaks. An increase in the radiating capacity of the outer casings from 0.85 to 0.87 also leads to a decrease in the maximum temperatures.

Thus, the mathematical distributed-lumped parameter model of heat transfer developed by us allows one to determine the basic pattern and main parameters of nonstationary heat transfer in the unusual U-shaped block of the service-system module including a passive thermal-regulation system based on nonregulated low-temperature heat pipes

of the unpressurized device compartment of a promising geostationary long-service-life spacecraft operating in the orbiting regime.

NOTATION

a, thermal diffusivity, m^2/sec; A, integral (total) hemispherical absorptivity; $Bi_{f.h} = \alpha_{f.h}\delta_h/\lambda_{eff}$, Biot number of the contact heat exchange through the adhesive joint between the casing and the honeycomb filler; c and C, specific and total heat capacities, J/(kg·K) and J/K; E_r, density of the net radiative heat flux, W/m^2; F, area, m^2; h, height, m; L_x, L_y, linear sizes of a panel, m; n, outer normal; $N_{h.p}$ and $N_{s.e}$, number of heat pipes and airborne-equipment devices; N_x, N_y, number of nodes into which a three-layer panel is divided on the axes of the Cartesian coordinate system; P, heat power released by a device, W; q, density of a heat flux, W/m^2; Q_m, source term in (2), K/sec; S_0, density of a direct solar-radiation flux, W/m^2; t, time, sec; T, temperature, K; $\bar{T}$, mean-integral temperature, K; x, y, Cartesian coordinates, m; α, coefficient of contact heat conductivity, $W/(m^2 \cdot K)$; B, boundary; δ, thickness, m; ε, integral (total) hemispherical radiating capacity; θ, angle between the normal to the device-radiator "north" and "south" panels and the direction to the Sun; λ, heat-conducting coefficient, W/(m·K); ρ, density, kg/m^3; ξ, march coordinate along the perimeter (a carcass element) of a honeycomb panel, m; σ, heat conduction, W/K; σ_0, Stefan–Boltzmann constant, $W/(m^2 \cdot K^4)$; Φ_m, $\Phi_{m\text{cont}}$, source terms in (3), K/sec. Subscripts: cont, contact between the two honeycomb panels of the carcass; cond, conductive; c, condensation zone; eff, effective; ES, shady region of the Earth; e, evaporation zone; f, casing; f.h, contact of the casing with the honeycomb filler; f.st, contact of the casing with the carcass elements; f.p, contact of the casing with the heat pipes; h, honeycomb filler; h.p, heat pipe; i, ordinal number of a computational node; int, initial conditions; m, ordinal number of a neighboring computational node; n, ordinal number of a heat-pipe unit in the evaporation (condensation) zone; p.p, contact of two heat pipes; s.e, airborne-equipment device; st, carcass element; s, direct solar radiation; v, saturated vapor; 1, 2, supporting casings; 3, 4, 5, 6, elements of the carcass of a three-layer honeycomb panel; 1, 2, 3, heat pipes in the "south," "central," and "north" panels in (14)–(19).

REFERENCES

1. E. A. Ashurkov, V. P. Kozhukhov, A. G. Kozlov, E. N. Korchagin, V. V. Popov, and M. F. Peshetnev, *Spacecraft of a Block-Module Design*, Patent 2092398 MKI B6461/10, Published 10.10.97. Byull. No. 28.
2. V. A. Burakov, E. N. Korchagin, V. P. Kozhukhov, et al., Mathematical simulation of heat exchange in an unpressurized device compartment of a spacecraft, *Inzh.-Fiz. Zh.*. **73**, No. 1, 113–124 (2000).
3. B. M. Pankratov, *Thermal Design of Aircraft Aggregates* [in Russian], Mashinostroenie, Moscow (1981).
4. N. N. Yanenko, *Subincremental Method of Solving Multidimensional Problems of Mathematical Physics* [in Russian], Nauka, Novosibirsk (1967).
5. A. A. Samarskii, *Theory of Difference Schemes* [in Russian], Nauka, Moscow (1982).